

Electrochemistry of Electron-Transfer Probes. The Role of the Leaving Group in the Cleavage of Radical Anions of α -Aryloxyacetophenones¹

Mogens L. Andersen, N. Mathivanan, and Danial D. M. Wayner*

Contribution from the Steacie Institute for Molecular Sciences, National Research Council of Canada, Ottawa, Ontario, Canada K1A 0R6

Received December 6, 1995[⊗]

Abstract: The formal reduction potential (E°) of α -phenoxyacetophenone has been determined from the voltammetric peak potential obtained by linear sweep voltammetry in combination with the rate constant for fragmentation of the radical anion which had been determined by laser flash photolysis. The E° values of a number of α -aryloxyacetophenones were then estimated from a correlation of the ¹³C chemical shifts of the carbonyl carbon and a similar correlation (E° versus ¹³C chemical shift) within a series of substituted α -anilinoacetophenones. Using these potentials (which vary by only 34 mV over a wide range of substituents) the rate constants for fragmentation of the α -aryloxyacetophenone radical anions were determined from digital simulation of the corresponding voltammetric waves. The fragmentation rate constants were shown to correlate with the pK_a of the corresponding phenols. However, the kinetic range was too small and the experimental errors too large to allow a distinction between a linear and quadratic free energy dependence. A thermochemical analogy between the leaving group ability in reactions of radical anions and that in simple heterolysis of closed shell compounds is developed. The utility of these compounds as potential electron transfer probes is discussed.

Introduction

Although the formation and subsequent fragmentation of radical anions ($RX^{\bullet-}$) are important processes in connection with the $S_{RN}1$ mechanism,^{2–7} only a few systematic studies of the absolute kinetics of these reactions have been reported.^{8–11} Recent work by Maslak¹² showed that the rate constant for fragmentation of radical ions of some substituted 1,2-diarylethanes followed a Marcus-like relationship and reached a limiting value when the driving force was very large. This somewhat empirical approach has been addressed more quantitatively by Savéant, who derived a theory, based on his theory of dissociative electron transfer^{13,14} (which in turn is an extension of Marcus theory), that treats the fragmentation essentially as an intramolecular dissociative electron transfer.¹⁵ This approach has been successful for a number of cases in which the thermodynamic driving forces for the reactions of interest are well-known or easily estimated using thermochemical cycles. However, the use of thermochemical cycles is often limited as they require knowledge of the standard potential (E°) of RX ,

which is difficult to obtain when the fragmentation is fast. In addition, the homolytic bond dissociation free energy (BDFE) of RX in solution, which also is required, is usually estimated from gas-phase enthalpy data.

Radical anion fragmentations also have been employed as mechanistic probes for electron transfer in studies of the competition between hydride and electron transfer in a number of organic^{16–18} and biological¹⁹ reduction reactions. In these experiments, observation of the fragmentation products was viewed as evidence for electron transfer. Since the electron transfer steps in all of these cases were known to be endergonic processes (i.e. the reverse reaction will be much faster than the forward), there have been a number of attempts to “calibrate” the mechanistic probes, by determining the rate constant for fragmentation of the radical anions.^{20–22} The ideal mechanistic probe is one in which the rate of oxidation of the radical anion (i.e. back electron transfer) cannot compete with fragmentation. Conceptually, this approach is analogous to the so-called free radical “clocks” which is now well-established in free radical chemistry.²³

One of the mechanistic probes used by Tanner and co-workers²⁰ is based on the fragmentation of the radical anion of α -phenoxyacetophenone. In this work the rate constant for the fragmentation was estimated from a product study in which the α -phenoxy fragmentation occurred in competition with the loss of halide ion from the acetophenone ring. Thermally and photochemically induced fragmentations of the C–O_{Ph} bond

[⊗] Abstract published in *Advance ACS Abstracts*, April 15, 1996.

(1) Issued as NRCC publication No. 39101.
 (2) Saveant, J.-M. *Tetrahedron* **1994**, *50*, 10117–10165.
 (3) Rossi, R. A.; de Rossi, R. H. *Aromatic Substitution by the $S_{RN}1$ Mechanism*; American Chemical Society: Washington, DC, 1983; Vol. 178.
 (4) Bowman, W. R. *Chem. Soc. Rev.* **1988**, *17*, 283–316.
 (5) Bunnett, J. F. *Acc. Chem. Res.* **1978**, *11*, 413–420.
 (6) Kornblum, N. *Angew. Chem., Int. Ed. Engl.* **1975**, *14*, 734.
 (7) Amatore, C.; Combella, C.; Pinson, J.; Oturan, M. A.; Robville, S.; Saveant, J.-M.; Thiebault, A. *J. Am. Chem. Soc.* **1985**, *107*, 4846–4853.
 (8) M'Halla, F.; Pinson, J.; Saveant, J. M. *J. Am. Chem. Soc.* **1980**, *102*, 4120–4127.
 (9) Neta, P.; Behar, D. *J. Am. Chem. Soc.* **1980**, *102*, 4798–4802.
 (10) Maslak, P.; Kula, J.; Chateaufneuf, J. E. *J. Am. Chem. Soc.* **1991**, *113*, 2304–2306.
 (11) Berenjian, N.; Utley, J. H. P. *J. Chem. Soc., Chem. Commun.* **1979**, 550–551.
 (12) Maslak, P.; Vallombroso, T. M.; William H.; Chapman, J.; Narvaez, J. N. *Angew. Chem., Int. Ed. Engl.* **1994**, *33*, 73–75.
 (13) Savéant, J.-M. *J. Am. Chem. Soc.* **1992**, *114*, 10595.
 (14) Savéant, J.-M. *J. Am. Chem. Soc.* **1987**, *109*, 6788.
 (15) Saveant, J.-M. *J. Phys. Chem.* **1994**, *98*, 3716–3724.

(16) Tanner, D. D.; Chen, J. J. *J. Org. Chem.* **1989**, *54*, 3842–3846.
 (17) Tanner, D. D.; Singh, H. K. *J. Org. Chem.* **1986**, *51*, 5182–5186.
 (18) Tanner, D. D.; Singh, H. K.; Kharrat, A.; Stein, A. R. *J. Org. Chem.* **1987**, *52*, 2142–2146.
 (19) Tanner, D. D.; Stein, A. R. *J. Org. Chem.* **1988**, *53*, 1642–1646.
 (20) Tanner, D. D.; Chen, J. J.; Chen, L.; Luelo, C. *J. Am. Chem. Soc.* **1991**, *113*, 8074–8081.
 (21) Tanko, J. M.; Drumright, R. E.; Suleman, N. K.; Branner, L. E., Jr. *J. Am. Chem. Soc.* **1994**, *116*, 1785–1791.
 (22) Tanko, J. A.; Larry E. Brammer, J.; Hervas, M.; Campos, K. *J. Chem. Soc., Perkin Trans. 2* **1994**, 1407–1409.
 (23) Griller, D.; Ingold, K. U. *Acc. Chem. Res.* **1980**, *13*, 317–323.

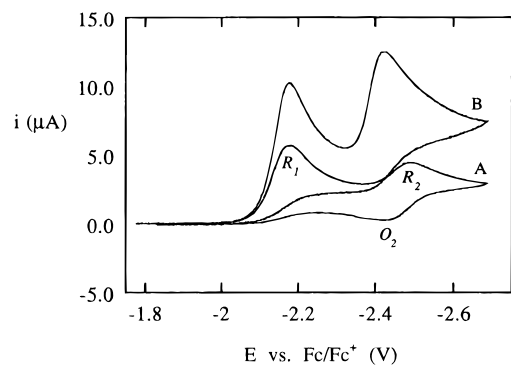
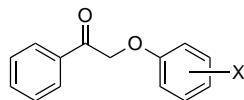


Figure 1. Cyclic voltammograms of (A) 1.9 mM α -phenoxyacetophenone (**Ia**) and (B) with 8.8 mM DBP added. DMF, 0.1 M TEAP, HMDE, sweep rate = 1 V·s⁻¹, *T* = 25 °C.

in other α -aryloxyacetophenones also have received considerable attention as it is believed that these are important reactions in the degradation of lignin,^{24–28} leading to the photoyellowing of paper. While most of the color reversion is thought to occur via photogenerated aryloxy radicals, lignin also contains alkoxystilbene substructures which can act as photoreductants.^{29,30} It is likely that some degradation of the lignin matrix occurs via the α -aryloxyacetophenone radical anions which are formed from a photoinduced electron transfer route in which electron-rich alkoxyl stilbenes are electron donors.

In this paper the kinetics of fragmentation of a number of α -aryloxyacetophenones (**Ia–h**) have been determined using electrochemical techniques in combination with laser flash photolysis data. Besides their importance as potential mechanistic probes and in the photodegradation of lignin, these radical anions are ideal for study of the relationship between the kinetics and the thermodynamics of the reactions since the nature of the leaving group can be systematically varied by substitution in the aryloxy ring.



- I**
- | | |
|----------------------|----------------------------------|
| a: X = H | e: X = <i>m</i> -CF ₃ |
| b: X = <i>m</i> -MeO | f: X = <i>p</i> -CF ₃ |
| c: X = <i>p</i> -MeO | g: X = <i>m</i> -CN |
| d: X = <i>m</i> -Cl | h: X = <i>p</i> -CN |

Results and Discussion

Cyclic Voltammetry and Coulometry. Cyclic voltammetry of **Ia–h** at a mercury working electrode (DMF/0.1 M tetraethylammonium perchlorate, TEAP) gave an irreversible wave (labeled R₁) and a reversible wave (labeled R₂/O₂) as seen, for example, for **Ia** in Figure 1. The reversible couple at R₂/O₂ is the reduction of acetophenone (*E*^o = -2.488V vs Fc/Fc⁺) and was observed in the cyclic voltammograms of all of the α -phenoxyacetophenones studied. In all cases, the reduction

(24) Vanucci, C.; Violet, P. F. D.; Bouas-Laurent, H.; Castellán, A. *J. Photochem. Photobiol., A: Chemistry* **1988**, *41*, 251–265.

(25) Schmidt, J. A.; Berinstain, A. B.; De Rege, F.; Heitner, C.; Johnston, L. J.; Scavano, J. C. *Can. J. Chem.* **1991**, *69*, 104–107.

(26) Wan, J. K. S.; Tse, M. Y.; Depew, M. C. *Res. Chem. Intermed.* **1992**, *17*, 59–75.

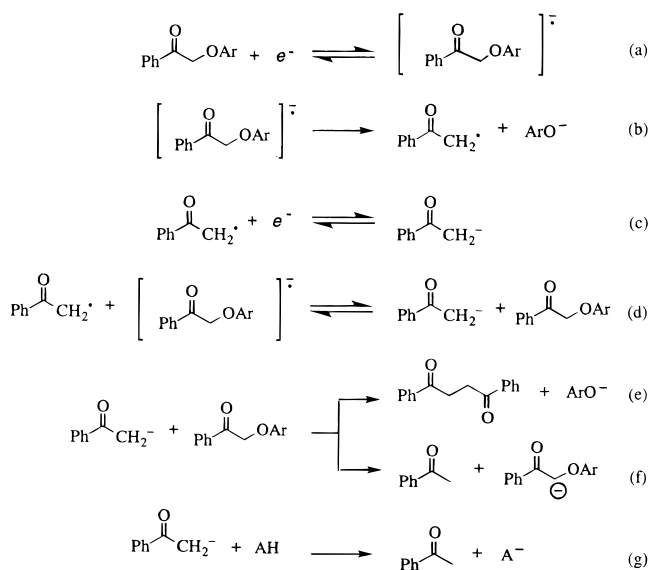
(27) Palm, W.-U.; Dreeskamp, H.; Bouas-Laurent, H.; Castellán, A. *Ber. Bunsenges. Phys. Chem.* **1992**, *96*, 50–61.

(28) Hurrell, L.; Johnston, L. J.; Mathivanan, N.; Vong, D. *Can. J. Chem.* **1993**, *71*, 1340–1348.

(29) Zhang, L.; Gellerstedt, G. *Acta Chem. Scand.* **1994**, *48*, 490–497.

(30) Wayner, D. D. M.; Luszyk, E.; Page, D.; Ingold, K. U.; Mulder, P.; Laarhoven, L. J. J.; Aldrich, H. S. *J. Am. Chem. Soc.* **1995**, *117*, 8737–8744.

Scheme 1



waves at R₁ were irreversible up to 1000 V/s. This is consistent with rate constants for the fragmentation of the radical anions > 1.0 × 10⁴ s⁻¹.³¹ The peak current for R₁ increased when 2,6-di-*tert*-butylphenol (DBP) was added to the solutions. A concurrent increase in the peak current for R₂ was also observed while the corresponding anodic peak, O₂, disappeared, indicative of protonation of the acetophenone radical anion (Figure 1b).

Constant current coulometry of **Ia** (2 mM) at a mercury pool cathode in DMF containing 0.1 M TEAP consumed 1.3 F/mol. The products obtained (HPLC and GC/MS) following acidification of the catholyte with acetic acid (AcOH) after 68% conversion of the α -phenoxyacetophenone (determined voltammetrically) were **Ia** (39%), acetophenone (31%), and 1,4-diphenyl-1,4-butadione (11%) (based on the initial concentration of substrate). In the presence of 6 mM AcOH the reduction of **Ia** consumed 2.0 F/mol, giving **Ia** (38%), acetophenone (41%), and 1,4-diphenyl-1,4-butadione (6%) after 58% conversion of **Ia**.

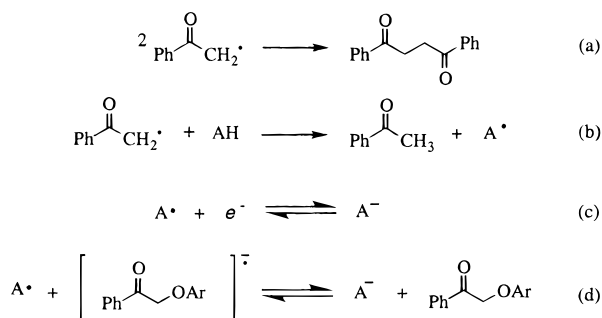
In the presence of 6 mM DBP, the amount of charge consumed was 2.1 (**Ia**), 2.0 (**Ic**), 2.2 (**Id**), and 2.0 F/mol (**Ih**). The catholytes in all of these four coulometry experiments were analyzed by HPLC after 60–70% conversion of the α -aryloxyacetophenones. It was found that in all four cases more than 90% of the consumed α -aryloxyacetophenone was converted into acetophenone and the corresponding phenol. 1,4-Diphenyl-1,4-butadione was not detected in any of these reaction mixtures. Added phenol has the same effect on the product distribution and the number of electrons transferred.³² However, the use of a hindered phenol in this study is necessary to avoid substitution reactions of **Ib–h**.

The voltammetric and coulometric observations can be understood by the mechanism in Scheme 1. The phenacyl radical which is formed after fragmentation of the radical anion (Scheme 1, reaction b) is more easily reduced than the neutral α -aryloxyacetophenones, leading to formation of the corresponding enolate. This second electron transfer occurs either directly at the electrode (ECE-type mechanism, Scheme 1, reaction c) or in solution by electron transfer from a radical anion (DISP-type mechanism, Scheme 1, reaction d). The enolate anion can subsequently react with a neutral substrate

(31) Mathivanan, N.; Johnston, L. J.; Wayner, D. D. M. *J. Phys. Chem.* **1995**, *99*, 8190–8195.

(32) Andrieux, C. P.; Savéant, J. M. *Bull. Chim. Soc. Fr.* **1972**, 3281–3290.

Scheme 2



molecule as a nucleophile leading to the formation of 1,4-diphenyl-1,4-butadiene (Scheme 1, reaction e) or it can react as a base and thus abstract a proton from the methylene group of the substrate (the so-called self protonation mechanism,³³ Scheme 1, reaction f). The latter reaction is thermodynamically favored since the pK_a values of **Ia** and acetophenone in DMSO are 21.1 and 24.7, respectively.³⁴ Thus, in the absence of acid, the overall reduction process consumes 2 electrons and 2 substrate molecules and therefore appears as a one-electron wave. Addition of acid intercepts the enolate anion (Scheme 1, reaction g) and an overall two electron wave is observed (Figure 1b).

The small amount of 1,4-diphenyl-1,4-butadiene that was formed when AcOH was used as acid indicates that some of the 1,4-diphenyl-1,4-butadiene must be formed through coupling of two phenacyl radicals (Scheme 2, reaction a). Acetic acid has a pK_a value of 12.3 in DMSO³⁴ and is expected to efficiently quench the acetophenone enolate. However, it is a poor hydrogen atom donor so it will not react with the phenacyl radicals. On the other hand, DBP is both a good proton donor (Scheme 1, reaction g) and a good hydrogen atom donor (Scheme 2, reaction b). This is consistent with the observation that 1,4-diphenyl-1,4-butadiene was not formed in the presence of DBP. If it is assumed that the yield of 1,4-diphenyl-1,4-butadiene formed in the presence of AcOH is a measure of the extent of radical-radical coupling, then only ca. 10% of the acetophenone formed in the presence of DBP is formed through this pathway.

In order to allow a more detailed analysis of the voltammetric waves, the acid used in this study must fulfill two requirements: (1) it must be strong enough to protonate the acetophenone enolate anions and (2) it cannot be so strong as to protonate the radical anion before it fragments. It is clear from the preceding discussion that the first requirement is met. That the second is met is easily demonstrated. Protonation of the radical anions results in the formation of ketyl radicals, which have been suggested to β -cleave to give the enol of acetophenone and phenoxy radicals,^{26,35,36} Scheme 3, and lead to the same products as predicted by Scheme 1. Thus, it is impossible to distinguish between these two cleavage routes from the product distribution. However, as seen from the data in Table 1 both the peak potentials and the half-peak widths, $E_{p/2} - E_p$, were independent of the DBP concentration for **Ia** and **Ih**, confirming that the reaction order of DBP must be zero³⁷ and, thus, ruling out the possibility that the radical anions are protonated by DBP.

(33) Amatore, C.; Capobianco, G.; Farnia, G.; Sandona, G.; Saveant, J.-M.; Severin, M. G.; Vianello, E. *J. Am. Chem. Soc.* **1985**, *107*, 1815–1824.

(34) Bordwell, F. G. *Acc. Chem. Res.* **1988**, *21*, 456–463.

(35) Scaiano, J. C.; Netto-Ferreira, J. C.; Wintgens, V. *J. Photochem. Photobiol. A: Chem.* **1991**, *59*, 265–268.

(36) Scaiano, J. C.; Whittlesey, M. K.; Berinstein, A. B.; Malenfant, P. R. L.; Shuler, R. H. *Chem. Mater.* **1994**, *6*, 836–843.

(37) Parker, V. D. In *Electroanalytical Chemistry*; Bard, A. J., Ed.; Marcel Dekker: New York, 1986; Vol. 14; pp 1–111.

Scheme 3

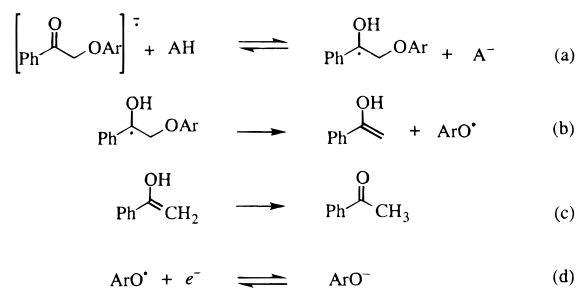


Table 1. The Effect of DBP on the Peak Potentials and Half-Peak Widths for the Reduction of α -Phenoxyacetophenones (2 mM) in DMF^a

[DBP], mM	Ia		Ih	
	E_p , V	$E_{p/2} - E_p$, mV	E_p , V	$E_{p/2} - E_p$, mV
2	-2.296	53.2	-2.095	56.6
4	-2.298	52.9	-2.093	58.0
8	-2.298	54.5	-2.093	56.8
20	-2.297	52.4	-2.093	58.0
40	-2.298	54.0	-2.090	58.1

^a 0.1 M TEAP, Hg electrode, $1 \text{ V}\cdot\text{s}^{-1}$, $T = 25 \text{ }^\circ\text{C}$. The values of E_p are versus the Fc/Fc^+ couple.

The peak potentials were studied as a function of the scan rate, v , for all the compounds up to 500 V s^{-1} and gave values of $\partial E_p/\partial \log(v)$ that were in the range 31 to 33 mV/decade (based on scan rates from 0.5 to $10 \text{ V}\cdot\text{s}^{-1}$).³⁸ This compares well with the theoretical value in the fast heterogeneous electron transfer limit of 29.6 mV/decade at $25 \text{ }^\circ\text{C}$.³⁹ However, at fast scan rates significant upward curvature toward the value for limiting heterogeneous electron transfer (59.1 mV/decade) is clear and suggests that in order to extract meaningful homogeneous rate constants (i.e. for the β -cleavage) care should be taken, at least at the fast scan rates, to consider the effect of the heterogeneous electron transfer on the voltammetric behavior.

At $1 \text{ V}\cdot\text{s}^{-1}$ the half-peak widths were in the range 52–59 mV, and they exhibited an increase upon increasing the sweep rate (the theoretical half-peak width in the fast heterogeneous electron transfer limit for the ECE and DISP mechanisms is 47.7 mV³⁹). This, again, suggests that the voltammetric peak potentials are at least partially controlled by the rate of the heterogeneous electron transfer. However, at these slow scan rates, the deviation from the theoretical value is small enough that the LSV-peak behavior will be determined principally by the cleavage of the radical anion.

The E° Value of **Ia.** The reduction of the α -aryloxyacetophenones was in all cases chemically irreversible on the time scale of the electrochemical experiments. Under these conditions it is possible to determine the rate constant for reaction of the radical anions from the observed peak potential if the standard potential, E° , is known, or conversely, the standard potential if the rate constant for fragmentation is known. Equation 1 describes the relationship between E_p and E° when the heterogeneous electron transfer can be described by the Nernst equation (m is a constant that depends on the mechanism (*vide infra*) and k is the unimolecular rate constant). However, the relationship between E_p and E° is more complex when the kinetics of the heterogeneous electron transfer contributes and digital simulation must be used to determine the relationship between E_p and E° .

(38) Andersen, M. L.; Wayner, D. D. M. *J. Electroanal. Chem.* In press.

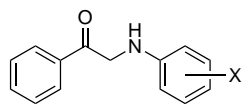
(39) Nadjo, L.; Saveant, J. M. *J. Electroanal. Chem.* **1973**, *48*, 113–145.

$$E_p = E^\circ - m \frac{RT}{F} + \frac{RT}{2F} \ln \left(\frac{RTk}{Fv} \right) \quad (1)$$

Recently, we reported a rate constant of $7 \times 10^5 \text{ s}^{-1}$ for the fragmentation of $\mathbf{Ia}^{\bullet-}$, in DMF, obtained by laser flash photolysis.³¹ In this study it was possible to determine cleavage rate constants only for $\mathbf{Ia}-\mathbf{c}^{\bullet-}$ (the others were too short lived) (Table 3). The LFP experiments also demonstrated that these rates of fragmentation were independent of the concentration of supporting electrolyte (up to 0.2 M).⁴⁰ Using this rate constant, it was possible to determine $E^\circ(\mathbf{Ia})$ by digital simulation of peak potentials and half-peak widths measured by LSV.³⁸ The simulations were based on a mixed ECE/DISP mechanism (consisting of reactions a–d in Scheme 1).⁴¹ The relative contribution of these two mechanistic extremes was determined by comparing the simulated peak potentials, $E_p - E^\circ$, and half-peak widths (obtained between 0.2 and 100 V/s in scan rate) with simulations based on either a pure ECE (reactions a–c in Scheme 1) or a pure DISP mechanism (reactions a, b, and d in Scheme 1). This simulation procedure leads to a standard potential of $-2.282 (\pm 0.005) \text{ V vs Fc/Fc}^+$ for \mathbf{Ia} in DMF (full details of the simulation procedure are published elsewhere).³⁸

It is interesting to compare the E° value for \mathbf{Ia} with the E° values for acetophenone ($-2.488 \text{ V vs Fc/Fc}^+$) and α -methoxyacetophenone ($-2.364 \text{ V vs Fc/Fc}^+$) which both give stable radical anions in DMF on the CV time scale and therefore allow a more reliable determination of their E° values. The trend that the α -phenoxy-substituted acetophenone is more easily reduced than the α -methoxy-substituted ketone, which in turn is more easily reduced than unsubstituted acetophenone, is consistent with the inductive effect of the substituents, phenoxy being more electron withdrawing than methoxy.

Estimation of Other E° Values Using Carbonyl ^{13}C Chemical Shifts. Analysis of the voltammograms for $\mathbf{Id}-\mathbf{h}$ is not straightforward since neither the homogeneous rate constant nor the standard potentials are known. However, the reduction of the nitrogen-containing analogues α -phenylaminoacetophenones ($\mathbf{IIa}-\mathbf{d}$) gave cyclic voltammograms consisting of a



X = H (**IIa**), *p*-MeO (**IIb**), *m*-CF₃ (**IIc**), *p*-CN (**IIId**)

reversible one electron couple and, thus, allowed the experimental determination of their E° values (see Table 2 and the Experimental Section for details). Changing the scan rates over at least one order of magnitude had no effect on the E° values, indicating that potential shifts caused by uncompensated resistance are negligible. Furthermore, these values were reproducible from day to day within a range of $\pm 3-4 \text{ mV}$.

While the respective radical anions of $\mathbf{IIa}-\mathbf{d}$ are much longer lived than the corresponding radical anions of $\mathbf{Ia}-\mathbf{h}$, the electronic effects of the remote substituents in these two groups of α -substituted acetophenones are expected to be similar. In both series of compounds the arylamino and the aryloxy groups

(40) Mathivanan, N.; Johnston, L. J.; Wayner, D. D. M. Unpublished results.

(41) The fact that 10% of the phenacyl radicals are abstracting a hydrogen atom from DBP instead of being reduced (reactions c and d in Scheme 1) is not expected to affect the LSV peak shapes, and thus the validity of using an ECE/DISP mechanism for the kinetic analysis. The hydrogen abstraction leads to the formation of a phenoxyl radical that is easily reduced either heterogeneously or homogeneously (reactions c and d in Scheme 2). Since these reactions are expected to be fast and, furthermore, take place after the rate determining cleavage of the anion radical, the electrochemical response will remain unchanged.

Table 2. Formal Reduction Potentials, E° , and ^{13}C Shift of Carbonyl Carbon of PhCOCH₂-Y-Ph-X

substituent X	Y = NH		Y = O	
	^{13}C shift, ^a ppm	E° , ^b V vs Fc/Fc ⁺	^{13}C shift, ^a ppm	E° , ^c V vs Fc/Fc ⁺
<i>p</i> -MeO	195.49	-2.350^e	194.60	-2.288 ± 0.006
H	195.01	-2.340^f	194.30	-2.282 ± 0.006^d
<i>m</i> -MeO			194.03	-2.276 ± 0.006
<i>m</i> -Cl			193.68	-2.269 ± 0.007
<i>m</i> -CF ₃	194.34	-2.327^f	193.51	-2.265 ± 0.008
<i>p</i> -CF ₃			193.56	-2.266 ± 0.008
<i>m</i> -CN			193.07	-2.256 ± 0.010
<i>p</i> -CN	193.62	-2.310^g	193.00	-2.254 ± 0.011

^a NMR shift of carbonyl carbon measured against TMS in CDCl₃.
^b DMF, 0.1 M TEAP, Hg electrode, $T = 25^\circ \text{C}$. The errors in the E° values are $\pm 3 \text{ mV}$.
^c Estimated from ^{13}C shift– E° correlation (see text). The errors quoted are based on eq 3.
^d Obtained by digital simulation of LSV results using the cleavage rate constant determined by LFP for the radical anion of \mathbf{Ia} (ref 27).
^e Reversible couple at sweep rates higher than $1 \text{ V}\cdot\text{s}^{-1}$.
^f Reversible couple at sweep rates higher than $5 \text{ V}\cdot\text{s}^{-1}$.
^g Reversible couple at sweep rates higher than $20 \text{ V}\cdot\text{s}^{-1}$.

interact with the benzoyl group through a methylene which attenuates the electronic interaction between the two halves of the molecules. Thus, the substituent effect on the relative stabilities of the neutral and charged species is transmitted by inductive (through the σ -bonds) or field (dipole–dipole) effects.^{42,43} The reduction potentials of the α -arylamino- and the α -aryloxyacetophenones are therefore expected to be determined primarily by the benzoyl group. This is clear from comparisons with the formal reduction potentials of *p*-cyanoaniline and *p*-cyanoanisole which were measured to be -3.194 and $-2.972 \text{ V vs Fc/Fc}^+$, respectively (DMF, 0.1 M TEAP), whereas the E° value for reduction of acetophenone is $-2.488 \text{ V vs Fc/Fc}^+$ under the same conditions. In addition, for $\mathbf{IIa}-\mathbf{d}$, the measured E° values change only by 40 mV with substitution from *para*-methoxy to *para*-cyano. Thus, the remote substituent effects are small compared to the effect of the α -heteroatom on the reduction potential of the acetophenone derivative (viz. the reduction potentials of \mathbf{Ia} and \mathbf{IIa} which are ca. 200 and 150 mV, respectively, more negative than that of acetophenone itself).

In principle, the E° values for the α -aryloxyacetophenones $\mathbf{Ia}-\mathbf{h}$ and the α -anilinoacetophenones $\mathbf{IIa}-\mathbf{d}$ should correlate with the ^{13}C chemical shifts of the carbonyl groups. The ^{13}C chemical shifts have been used as an indicator of charge density and of electronegativity of substituents. For $\mathbf{Ia}-\mathbf{h}$ and $\mathbf{IIa}-\mathbf{d}$ the ^{13}C chemical shift of the carbonyl carbon is only influenced by inductive effects from the α substituents (which are modulated by the remote substituent in the ring). In this case there is an upfield shift relative to the acetophenone value (197.92 ppm), Table 2, which is consistent with the phenoxy and anilino groups being electronegative.^{44,45} The ^{13}C chemical shifts of the carbonyl carbons in similarly substituted α -phenoxy- and α -phenylaminoacetophenones correlate linearly with each other with a slope of 0.892, Figure 2. The slope, which is less than unity, is consistent with the oxygen atom being less polarizable than the NH group.

It is reasonable to expect that the reduction potentials of structurally related aromatic ketones will correlate with the charge density of the carbonyl group which further implies that the reduction potentials should correlate with the ^{13}C chemical

(42) Brownlee, R. T. C.; Craik, D. J. *Org. Magn. Reson.* **1981**, *1981*, 248–256.

(43) Reynolds, W. F. *Prog. Phys. Org. Chem.* **1983**, *14*, 165–203.

(44) Olivato, P. R.; Bonfada, E.; Rittner, R. *Magn. Reson. Chem.* **1992**, *30*, 81–84.

(45) Duddeck, H. *Top. Stereochem.* **1986**, *16*, 219–324.

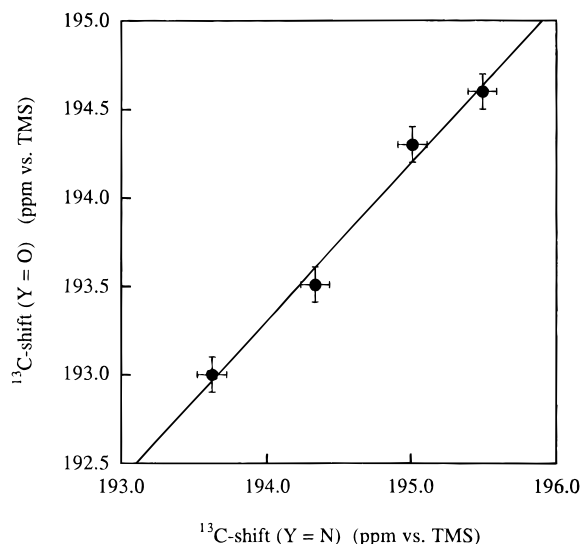


Figure 2. Correlation of ^{13}C shifts of carbonyl carbons in $\text{PhCOCH}_2\text{-Y-Ph-X}$. Data are taken from Table 2. The slope of the regression line is 0.892 (regression coefficient = 0.993).

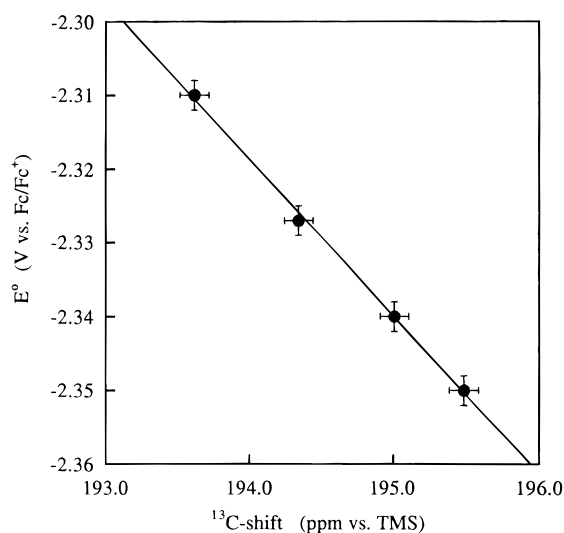


Figure 3. Linear correlation of ^{13}C shifts for carbonyl carbons and E° values for $\text{PhCOCH}_2\text{NHPh-X}$. Data are taken from Table 2. The slope of the regression line is -0.0212 V/ppm (regression coefficient = 0.999).

shifts of the carbonyl carbons. A plot of E° versus the carbonyl ^{13}C chemical shifts for **II** does indeed give an excellent linear correlation with a slope of -21 mV/ppm, Figure 3. If it is assumed that slopes of the linear correlations between the E° and the ^{13}C chemical shifts are the same for **I** and **II**, then it is possible to estimate the formal reduction potentials for **I** by using the E° value for **Ia** as the anchor point (eq 2).

$$E^\circ(\alpha\text{-phenoxyacetophenones}) = -2.282 - 0.021(\delta^{13}\text{C}(\text{ppm}) - 194.30) \quad (2)$$

The E° values estimated in this way are given in Table 2. It is noteworthy that the E° values are predicted to change by only 34 mV through the series of α -aryloxyacetophenones **Ia-h**, however, considering the somewhat empirical approach and the assumption that the slope of the line in Figure 3 can be applied to **I**. The errors in the E° values, $\sigma(E^\circ)$, calculated from eq 2 arise from the following: (1) the error in the E° value for **Ia**, $\sigma_{E^\circ(\text{Ia})}$, which has been estimated as ± 5 mV, (2) the errors in the ^{13}C shifts, $\sigma^{13}\text{C}$, which have been estimated to ± 0.1 ppm, and (3) the error in the slope, σ_{slope} , of the correlation in Figure

3 (eq 2). The possibility that the slopes of the α -anilinoacetophenone correlation and the α -phenoxyacetophenone correlation are not identical is included in the assessment of this error. However, the two series of compounds are structurally and electronically very closely related so it is likely that the slopes for these two series of compounds also are similar. However, in order to err on the side of caution, the error on the slope used in eq 2 has been set to $\pm 33\%$ of the slope from Figure 3 (i.e. ± 7 mV/ppm).

The error associated with the use of eq 2 can be calculated from eq 3. This equation is based on the assumption that the errors can be treated as standard deviations, and that the covariances can be neglected. The resulting errors are listed in Table 2. It is noteworthy that the largest error is ± 10 mV, which will result in an error of a factor of only two in rate constants derived from electrochemical data based on these E° values.

$$\sigma_{E^\circ} = \{ \sigma_{E^\circ(\text{Ia})}^2 + (\delta^{13}\text{C} - 194.30)^2 \sigma_{\text{slope}}^2 + (0.0212)^2 \sigma^{13\text{C}}{}^2 \}^{1/2} \quad (3)$$

Kinetics of Fragmentation of Radical Anions. Since the E° values can be reasonably estimated, it is possible to determine the rate constants for fragmentation from voltammetric peak potentials, E_p . If the rate of the heterogeneous electron transfer is fast (i.e. the rate determining step is the homolytic cleavage of the radical anion at scan rates < 1 V s^{-1}), then eq 1 can be used to calculate the rate constants in the case of both the ECE ($m = 0.78$) and DISP ($m = 1.127$) variants of the mechanism.⁴⁶ The use of this equation, however, can lead to a significant underestimate of the rate constants when the rate of the heterogeneous electron transfer is not fast enough to be ignored (i.e. mixed kinetic control or rate determining heterogeneous electron transfer).^{21,39} This situation can arise at scan rates > 10 V s^{-1} when the homogenous reaction becomes so fast ($k > 10^5$ s^{-1}) that even heterogeneous electron transfer rates normally considered to be fast (i.e. 1 to 3 $\text{cm}^2 \text{s}^{-1}$) are competitive with or are even slow on the time scale of the homogeneous process.

For the reduction of **Ia-h**, the values of the half-peak widths and $\partial E_p / \partial \log(v)$ measured by LSV indicate the reductions are, in fact, under mixed control (vide supra). At the slowest scan rates eq 1 is probably a reasonable approximation. However, it is preferable to find a single set of parameters that fit the data at all scan rates. Under these conditions, the extraction of the homogeneous rate constant is more complicated and requires an iterative approach using a digital simulation procedure that takes both the heterogeneous electron transfer rate and the possibility of a mixed ECE/DISP mechanism into account. The same digital simulation procedure as was used for the determination of the E° value for **Ia** (see above) was also used to calculate the fragmentation rates of the radical anions of **Ib-h**, with the only difference being that in this case the simulations were based on the E° values given in Table 2.³⁸ The results of this treatment are given in Table 3. A comparison of the experimental data with results from digital simulation for **Ig** is shown in Figure 4 together with simulated working curves for both the DISP and ECE mechanisms. The heterogeneous electron transfer rates, also determined from the iterative approach, were found to be in the range of 1–2 $\text{cm}^2 \text{s}^{-1}$ which is typical for fast heterogeneous electron transfer to organic molecules of this general class at a mercury electrode.⁴⁷ In the case of **Ib** and **Ic**, the rate constants measured by laser flash photolysis (1×10^6 and 4×10^5 s^{-1} respectively)³¹ are in

(46) Amatore, C.; Saveant, J. M. *J. Electroanal. Chem.* **1977**, *85*, 27–46.

(47) Kojima, H.; Bard, A. J. *J. Am. Chem. Soc.* **1975**, *97*, 6317–6324.

Table 3. Rate Constants and Mechanisms for the Fragmentation of Radical Anions of **Ia–h** in DMF^a

substituent	$k,^b \text{ s}^{-1}$	mechanism
<i>p</i> -MeO	$3.8 \times 10^5 (4 \times 10^5)^c$	DISP
H	$-(7 \times 10^5)^c$	DISP
<i>m</i> -MeO	$1.2 \times 10^6 (1 \times 10^6)^c$	DISP
<i>m</i> -Cl	2.1×10^7	ECE/DISP
<i>m</i> -CF ₃	2.1×10^7	ECE/DISP
<i>p</i> -CF ₃	4.0×10^7	ECE/DISP
<i>m</i> -CN	6.3×10^7	ECE/DISP
<i>p</i> -CN	2.8×10^8	ECE

^a 2 mM α -aryloxyacetophenone, 10 mM DBP, 0.1 M TEAP, Hg electrode, $T = 25^\circ\text{C}$. ^b The error in $\log(k)$ is estimated to be ± 0.3 (see text). ^c Measured by laser flash photolysis in DMF (ref 27).

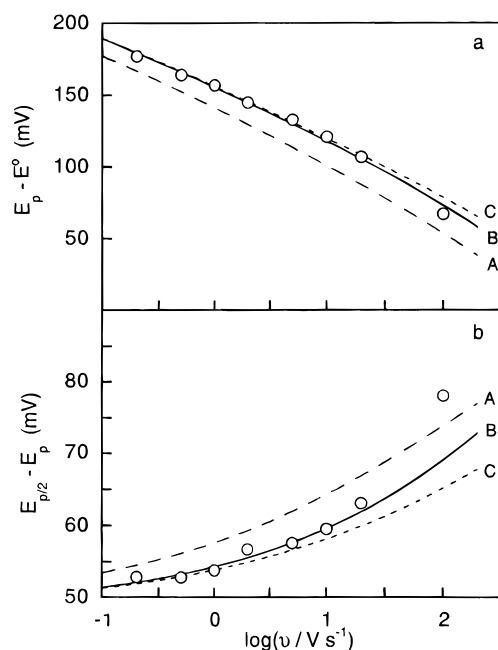


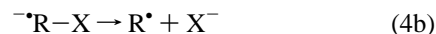
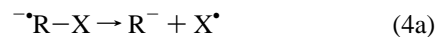
Figure 4. Experimental and digitally simulated peak shifts (a) and half peak widths (b) for **Ig**. $k = 7 \times 10^7 \text{ s}^{-1}$, $k^0 = 2.0 \text{ cm}^2 \text{ s}^{-1}$, and $E^0 = -2.256 \text{ V vs Fc/Fc}^+$. (A) DISP mechanism. (B) ECE/DISP mechanism. (C) ECE mechanism.

excellent agreement with the values determined by the digital simulation procedure from the voltammetric data. Interestingly, the change in fragmentation rates is large enough that the reduction mechanism passes from a DISP type to an ECE type over the range of substituents used; i.e. as the lifetimes of the radical anions become shorter the fragmentation takes place closer to the electrode so that direct reduction of the radical at the electrode becomes kinetically more favorable. The competitive ECE/DISP kinetic behavior is evident for **Ig** as seen in Figure 4.

The error of $\pm 10 \text{ mV}$ in the estimated E^0 values is the main source of error in the calculated values of k , and it results in an error equal to ± 0.3 in the calculated values of $\log(k)$. However, the errors in $\log(k)$ for **Ia–c**,³¹ which have been determined by LFP, are estimated to be only ± 0.08 .

Thermochemical Considerations. The fragmentation of radical anions, $\text{RX}^{\bullet-}$, in which the SOMO is essentially localized on the R moiety (in this case phenacyl), can formally take place either as a homolysis (reaction 4a) or as a heterolysis (reaction 4b) route.^{12,48} Since, for the radical anions **Ia–h**^{•-}, the substituents have essentially no effect on the energy of the radical anion relative to the neutral (i.e. the E^0 values are essentially constant), the changes in the activation free energies (kinetics)

should be determined by the relative free energies of the fragment X (either as an anion or radical) since the fragment, R, will always be the same.



Similar free energy relationships have been observed for the fragmentation of a number of other chemical systems. For example, linear correlations between the logarithm of the heterolytic cleavage rate constant and the driving force have been found for alkyl chlorides in super acid media.⁴⁹ On the other hand, a quadratic relationship was found by Maslak and co-workers for the cleavage of radical ions of bibenzyl compounds,¹² and similarly, Savéant has developed a Marcus-type model for the cleavage of radical ions¹⁵ which also predicts a quadratic relationship. In the present case, the small kinetic range does not allow the distinction between a linear and a quadratic relationship.

Consideration of thermodynamics can give some insight into whether the fragmentation of **Ia–h**^{•-} occurs via the homolytic (reaction 4a) or heterolytic (reaction 4b) route. Homolysis leads to the formation of the enolate anion of acetophenone and a substituted phenoxy radical. The latter species is easily reduced to phenolate ions at the potentials where the corresponding α -aryloxyacetophenones are reduced.⁵⁰ Thus, this mechanism leads to the same products as that in Scheme 1. The free energy of the homolytic fragmentation of the radical anions, $\Delta G_{\text{hom}}^{\circ}(\text{RX}^{\bullet-})$, can be calculated from eq 5.⁵¹

$$\Delta G_{\text{hom}}^{\circ}(\text{RX}^{\bullet-}) = \text{BDFE}(\text{RX}) + FE^{\circ}(\text{RX}) - FE^{\circ}(\text{R}^{\bullet}) \quad (5)$$

In the present case the R moiety is always phenacyl so the reduction potential $E^{\circ}(\text{R}^{\bullet})$ is constant. Since $E^{\circ}(\text{RX})$ changes by less than 40 mV (ca. 1 kcal/mol), the second term in the equation also can be considered to be constant. The substituent effect on the driving force for the homolytic cleavage (reaction 4a) is, therefore, expected to depend only on the free energy of the homolytic bond cleavage of the neutral α -aryloxyacetophenone, $\text{BDFE}(\text{RX})$. If the reasonable assumption is made that the entropy change associated with the fragmentation is the same for all the compounds, then the free energy of cleavage of the radical anion will depend only on the bond dissociation energy (BDE) of the C–O bond of the neutral RX. As BDE's for the O–H bonds in 4-substituted phenols^{52,53} and the O–Me bonds in anisoles⁵⁴ correlate with σ^+ (with the electron-donating substituents having the smallest BDE's), it is reasonable to expect the same to be the case for the α -aryloxyacetophenones. However the fragmentation rates are observed to increase as the electron demand of the substituent increases which is not consistent with homolysis of the C–O bond in **Ia–h**^{•-}. It is noteworthy in this connection that the rate constants for the fragmentation of triplet α -aryloxyacetophenones are consistent with loss of aryloxy radicals and decrease as the electron

(49) Arnett, E. M.; Petro, C.; Schleyer, P. v. R. *J. Am. Chem. Soc.* **1979**, *101*, 522–526.

(50) Hapiot, P.; Pinson, J.; Yousfi, N. *New. J. Chem.* **1992**, *16*, 877–881.

(51) Wayner, D. D. M.; Parker, V. D. *Acc. Chem. Res.* **1993**, *26*, 287–294.

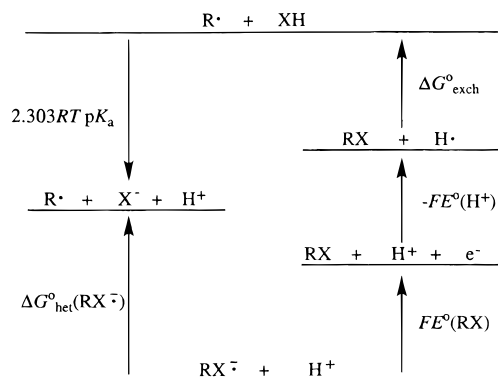
(52) Mulder, P.; Saastad, O. W.; Griller, D. *J. Am. Chem. Soc.* **1988**, *110*, 4090–4092.

(53) Lind, J.; Shen, X.; Eriksen, T. E.; Merenyi, G. *J. Am. Chem. Soc.* **1990**, *112*, 479–482.

(54) Surayan, M. M.; Kafafi, S. A.; Stein, S. E. *J. Am. Chem. Soc.* **1989**, *111*, 4594–4600.

(48) Maslak, P.; Guthrie, R. D. *J. Am. Chem. Soc.* **1986**, *108*, 2628–2636.

Scheme 4



demand of the substituent increases.⁵⁵ Interestingly, thermochemical considerations suggest that the homolytic fragmentation is the preferred mode of cleavage only for **1c**^{•-}.⁵⁶

The thermochemistry of the heterolytic cleavage of radical anions (reaction 4b) can be calculated from the thermochemical cycle in Scheme 4. This thermochemical cycle for the cleavage of radical anions is based on pK_a values of acids of the corresponding leaving group, X. The free energy relationship that defines the fragmentation of the radical anion, $\Delta G^\circ_{\text{het}}(\text{RX}^{\bullet-})$, is given in eq 6, where $\Delta G^\circ_{\text{exch}}$ is defined as the difference between the bond dissociation free energy of R–X and that of H–X (eq 7).

$$\Delta G^\circ_{\text{het}}(\text{RX}^{\bullet-}) = 2.303RTpK_a(\text{HX}) + FE^\circ(\text{RX}) - FE^\circ(\text{H}^+) + \Delta G^\circ_{\text{exch}} \quad (6)$$

$$\Delta G^\circ_{\text{exch}} = \text{BDFE}(\text{RX}) - \text{BDFE}(\text{HX}) \quad (7)$$

Since $E^\circ(\text{H}^+)$ and $E^\circ(\text{RX})$ are constant in the present case this equation predicts a Brønsted-type relationship as long as $\Delta G^\circ_{\text{exch}}$ is either constant or also follows a Brønsted-type relationship; i.e. under these conditions, $\Delta\Delta G^\circ_{\text{het}}(\text{RX}^{\bullet-}) = \Delta pK_a$. In fact, a Brønsted-type plot (Figure 5) shows that a linear correlation exists between $\log(k)$ and the pK_a of the corresponding phenol. Thus, the relative kinetic data are consistent with heterolysis of the C–O bond in the fragmentation of **1a–h**^{•-} (reaction 4b). The pK_a values for the phenols in DMF that have been used in Figure 5 are calculated from the corresponding values in DMSO⁵⁷ by using the following empirical relationship: $pK_a(\text{DMF}) = 1.56 + 0.96pK_a(\text{DMSO})$.^{58,59}

(55) Netto-Ferreira, J. C.; Avelar, I. G. J.; Scaiano, J. C. *J. Org. Chem.* **1990**, *55*, 89–92.

(56) The difference in free energy between the homolytic cleavage (reaction 5) and the heterolytic cleavage (reaction 6) of radical anions is equal to the difference in reduction potentials of X^\bullet and R^\bullet , i.e. $\Delta\Delta G^\circ = -F[E^\circ(\text{R}^\bullet) - E^\circ(\text{X}^\bullet)]$. The peak potential of the irreversible oxidation of $\text{C}_6\text{H}_5\text{COCH}_2^\bullet$ in DMSO is -0.54 V vs Fc/Fc^+ (Bordwell, F. G.; Harrelson, J. A., Jr. *Can. J. Chem.* **1990**, *68*, 1714). This value can be converted to an E° value equal to -0.34 V vs Fc/Fc^+ in DMF if it is assumed it to be kinetically shifted by ca. 200 mV from $E^\circ(\text{C}_6\text{H}_5\text{COCH}_2^\bullet)$ (Wayner, D. D. M.; Parker, V. D. *Acc. Chem. Res.* **1993**, *26*, 287) and that the E° value is the same in DMF and DMSO. The E° values for the reversible oxidation of 4-substituted phenolates in MeCN have been found to give a linear correlation with σ^+ (Hapiot, P.; Pinson, J.; Yousfi, N. *New J. Chem.* **1992**, *16*, 877). Using this correlation results in $E^\circ(\text{C}_6\text{H}_5\text{O}^\bullet) = -0.19$ V vs Fc/Fc^+ and $E^\circ(p\text{-MeO-C}_6\text{H}_4\text{O}^\bullet) = -0.65$ V vs Fc/Fc^+ . If it is assumed that these values do not change on going from MeCN to DMSO, $\Delta\Delta G^\circ$ is found to be 3.5 kcal/mol for X = PhO, and -7.1 kcal/mol for X = *p*-MeO-C₆H₄O. These free energies suggest that only in the case of **1c** is the fragmentation of the radical anion expected to follow the homolytic route; the anion radicals of the other α -phenoxyacetophenones follow the heterolytic route since E° for the reduction of their corresponding phenoxy radicals are more positive than $E^\circ(p\text{-MeO-C}_6\text{H}_4\text{O}^\bullet)$ values.

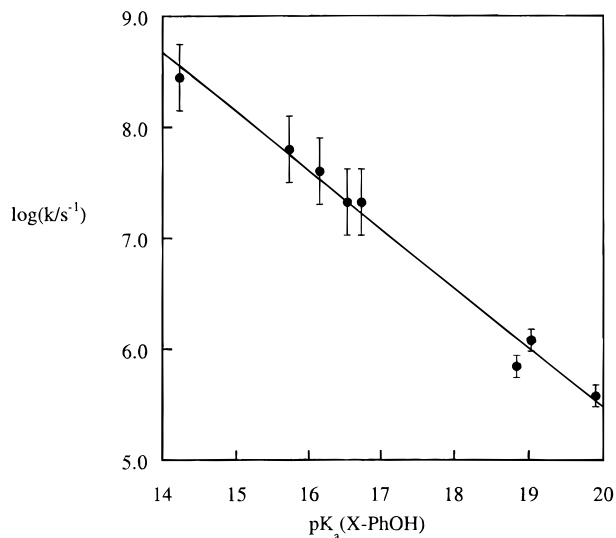


Figure 5. Brønsted-type plot of the cleavage rate constants of the α -phenoxyacetophenones plotted versus the pK_a value of the corresponding phenol. The slope of the regression line is 0.53 (regression coefficient = 0.993).

At present there are no experimental data in the literature that allow the effect of substitution on the phenoxy ring on $\Delta G^\circ_{\text{exch}}$ to be evaluated. Data for O–Me bond strengths in anisoles⁵⁴ and O–H bond strengths in phenols⁵² suggest that there may be a small effect. However, the anisole data were obtained in the gas phase whereas the phenol data were obtained in solution. Hydrogen bonding to the solvent has been shown to affect BDE of phenol in solution³⁰ which makes it difficult to compare the two sets of data directly. If we make the assumption that both $E^\circ(\text{RX})$ and $\Delta G^\circ_{\text{exch}}$ are constant in eq 6, then the slope, α , of the linear regression line in Figure 5 is simply a Brønsted coefficient since $\alpha = -\partial\log(k)/\partial pK_a \approx \partial\Delta G^\circ/\partial\Delta G^\circ$. It is noteworthy that the slope of the regression line in Figure 5 is 0.53 which is close to 0.5, the value expected for reaction with a symmetrical transition state near $\Delta G = 0$ (e.g. $\Delta G_{\text{X-H}} \approx -4$ kcal mol⁻¹).

The observation that the leaving group ability in the fragmentation of both radical anions and closed shell compounds (e.g. in $\text{S}_{\text{N}}1$ and E1 reactions)^{60,61} depends on the pK_a value of the corresponding acid HX is easily rationalized. An analogous thermochemical cycle can be constructed for the free energy, $\Delta G^\circ_{\text{het}}(\text{RX})$, of heterolytic bond cleavage in neutral molecules (Scheme 5 and eq 8). The form of eq 8 is similar to that of eq 6 inasmuch as they both depend on the pK_a of XH and $\Delta G^\circ_{\text{exch}}$

(57) Bordwell, F. G.; Cheng, J.-P. *J. Am. Chem. Soc.* **1991**, *113*, 1736–1743.

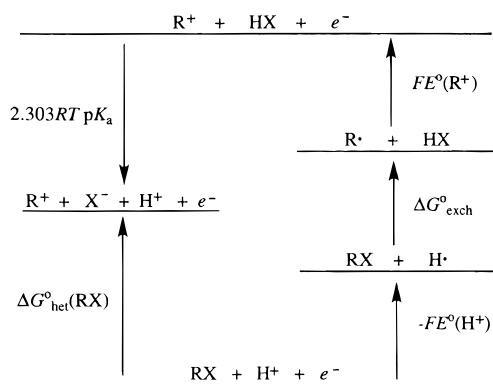
(58) Maran, F.; Celadon, D.; Severin, M. G.; Vianello, E. *J. Am. Chem. Soc.* **1991**, *113*, 9320–9329.

(59) It is interesting to note that the pK_a reported for *m*-methoxyphenol in DMSO is 0.2 pK_a units higher than the pK_a value for the unsubstituted phenol in contradiction to the weak electron withdrawing nature of this *meta* substituent. It is possible that this anomalous pK_a value is the reason for the deviation of the points corresponding to **1a–c** in Figure 5. The pK_a value for *m*-methoxyphenol has been found to be 0.7 pK_a unit lower than the phenol value in DMSO by using a potentiometric method (Kalfus, K.; Socha, J.; Vecera, M. *Collect. Czech. Chem. Commun.* **1974**, *39*, 275). Lowering the pK_a value for *m*-methoxyphenol by 0.7 pK_a unit would place the point corresponding to **1b** on the regression line in Figure 5. However, even though the pK_a value for *m*-methoxyphenol reported in DMSO appears to be too high, we have chosen to use the data from ref 52 since they represent the only complete set that have been obtained (by a spectrophotometric method) against the same set of indicators. Furthermore, this set of values has been corrected for contributions from homo-hydrogen bonding.

(60) Arnett, E. M.; Chawla, B.; Molter, K.; Amarnath, K.; Healy, M. J. *Am. Chem. Soc.* **1985**, *107*, 5288–5289.

(61) Lowry, T. H.; Richardson, K. S. *Mechanism and Theory in Organic Chemistry*, 3rd ed.; Harper & Row Publishers: New York, 1987.

Scheme 5



in addition to a standard potential of either a reactant or product. The relationship between the heterolysis of RX and its corresponding radical anion is given in eq 9. The often dramatic weakening of the RX bond upon one-electron reduction is simply related to the fact that $E^\circ(\text{R}^+)$ is generally much greater than $E^\circ(\text{RX})$.⁵¹

$$\Delta G^\circ_{\text{het}}(\text{RX}) = 2.303RTpK_a + FE^\circ(\text{R}^+) - FE^\circ(\text{H}^+) + \Delta G^\circ_{\text{exch}} \quad (8)$$

$$\Delta G^\circ_{\text{het}}(\text{RX}^{\bullet-}) - \Delta G^\circ_{\text{het}}(\text{RX}) = FE^\circ(\text{RX}) - FE^\circ(\text{R}^+) \quad (9)$$

Conclusions

The formal reduction potentials of the α -phenoxyacetophenones **1a–h** have been estimated by using the ^{13}C chemical shifts of the carbonyl carbons as a measure of the charge density of the acetophenone moiety and by comparing these properties with those for the corresponding α -anilinoacetophenones which form long-lived radical anions on the time scale of the voltammetric experiments. The kinetics of the fragmentation of the radical anions **1a–h**⁻ were determined by digital simulation of voltammetric waves obtained by LSV measurements in combination with some data obtained by laser flash photolysis. The rate constants cover a range of almost three orders of magnitude even though the reduction potentials of the neutral precursors only vary by ca. 34 mV. These fragmentation rates are shown to correlate with the pK_a values (which, in fact, reflect changes in the thermodynamic driving force) of the corresponding phenols. However, the small kinetic range in the data does not allow one to distinguish between the linear and quadratic free energy relationships (although the most reliable theory¹⁵ predicts a quadratic dependence).

The data herein suggest that it should be possible to design an electron-transfer probe with predetermined thermodynamic and kinetic properties. Judicious choice of substituents allows the design of a probe in which the radical anion fragments on a time scale from seconds to sub-nanoseconds. The present case is particularly interesting in that the lifetime of the radical anion was varied from ca. 2 μs to ca. 30 ns while the thermodynamics (and presumably kinetics) of its formation was essentially constant. This work is being extended to include the effect of substitution on the acetophenone ring in order to increase the kinetic range for studies of the free energy relationships.

Finally, the thermochemistry of the cleavage process, estimated from thermochemical cycles, predicts that the free energy of the fragmentation of $\text{RX}^{\bullet-}$ should depend on the $pK_a(\text{HX})$ of the leaving group (X^-) and the difference between the homolytic bond dissociation energies of $\text{H}-\text{X}$ and $\text{R}-\text{X}$. An analogous thermochemical relationship also is shown to exist

for simple heterolytic cleavage reactions (i.e. $\text{S}_{\text{N}}1$) of closed shell compounds. Thus, the change in the leaving group abilities of a series X^- from a neutral RX compared to its radical anion, from a thermochemical viewpoint, only depends on the standard potential of RX (i.e. R^+ is constant, eq 9). This relationship can be used to explore the question of whether kinetics for loss of X^- from a $\text{RX}^{\bullet-}$ and RX follow the same free energy relationship (i.e. have the same intrinsic barriers) and, possibly, to extend the scale leaving group abilities to include leaving groups that are not sufficiently reactive in conventional approaches.

Experimental Section

DMF was distilled from CaH_2 under argon at a reduced pressure. TEAP (Kodak) was recrystallized three times from ethanol/water. 2,6-Di-*tert*-butylphenol (Aldrich) was recrystallized at least twice from hexane or ethanol. α -Phenoxyacetophenones (**1a–h**) were synthesized according to the literature procedure.⁵⁵

α -(*m*-Methoxyphenoxy)acetophenone (1b**):** mp 85 °C. ^1H NMR (400 MHz, CDCl_3) δ 3.69 (s, 3H), 5.19 (s, 2H), 6.48–6.51 (m, 3H), 7.12 (t, $J = 8$ Hz, 1H), 7.43 (t, $J = 8$ Hz, 2H), 7.55 (t, $J = 8$ Hz, 1H), 7.93 (t, $J = 8$ Hz, 2H). ^{13}C NMR (100 MHz, CDCl_3) δ 54.93 ($-\text{OCH}_3$), 70.34 (CH_2), 101.25, 106.34, 107.00, 127.76, 128.54, 129.73, 133.56, 134.25 (aromatic), 158.99 ($\text{C}-\text{OMe}$), 160.60 ($\text{C}-\text{OCH}_2$), 194.03 ($\text{C}=\text{O}$). MS (EI^+) m/z (%) 242 (34), 105 (100), 77 (37).

α -(*m*-(Trifluoromethyl)phenoxy)acetophenone (1e**):** mp 97 °C. ^1H NMR (400 MHz, CDCl_3) δ 5.33 (s, 2H), 7.09 (d, $J = 8$ Hz, 1H), 7.19 (s, 1H), 7.23 (d, $J = 8$ Hz, 1H), 7.37 (t, $J = 8$ Hz, 1H), 7.49 (t, $J = 8$ Hz, 2H), 7.62 (t, $J = 8$ Hz, 1H), 7.98 (d, $J = 8$ Hz, 2H). ^{13}C NMR (50 MHz, CDCl_3) δ 70.52 (CH_2), 111.83, 117.98, 118.20, 127.94, 128.85, 130.07, 134.01 (aromatic), 123.78 (q, $J = 272$ Hz, CF_3), 131.82 (q, $J = 33$ Hz, $\text{C}-\text{CF}_3$), 134.23 ($\text{C}-\text{C}=\text{O}$), 158.08 ($\text{C}-\text{OCH}_2$), 193.51 ($\text{C}=\text{O}$). MS (EI^+) m/z (%) 280 (8), 261 (4), 145 (7), 105 (100), 77 (35).

α -(*p*-(Trifluoromethyl)phenoxy)acetophenone (1f**):** mp 92 °C. ^1H NMR (400 MHz, CDCl_3) δ 5.33 (s, 2H), 6.99 (d, $J = 10$ Hz, 2H), 7.47–7.55 (m, 4H), 7.61 (t, $J = 7$ Hz, 1H), 7.97 (d, $J = 7$ Hz, 2H). ^{13}C NMR (50 MHz, CDCl_3) δ 70.46 (CH_2), 114.73, 127.00, 128.01, 128.94, 134.13 (aromatic), 124.27 (q, $J = 272$ Hz, CF_3), 123.76 (q, $J = 33$ Hz, $\text{C}-\text{CF}_3$), 134.24 ($\text{C}-\text{C}=\text{O}$), 160.39 ($\text{C}-\text{OCH}_2$), 193.56 ($\text{C}=\text{O}$). MS (EI^+) m/z (%) 280 (7), 261 (3), 145 (6), 105 (100), 77 (35).

α -(*m*-Cyanophenoxy)acetophenone (1g**):** mp 87 °C. ^1H NMR (400 MHz, CDCl_3) δ 5.33 (s, 1H), 7.14–7.17 (m, 2H), 7.25 (d, $J = 8$ Hz, 1H), 7.36 (t, $J = 8$ Hz, 1H), 7.51 (t, $J = 8$ Hz, 2H), 7.63 (t, $J = 8$ Hz, 1H), 7.96 (d, $J = 8$ Hz, 2H). ^{13}C NMR (50 MHz, CDCl_3) δ 70.33 (CH_2), 113.02 ($\text{C}-\text{CN}$), 118.35 (CN), 117.69, 119.75, 125.09, 127.76, 128.79, 130.31, 134.02 (aromatic), 133.91 ($\text{C}-\text{C}=\text{O}$), 157.95 ($\text{C}-\text{OCH}_2$), 193.07 ($\text{C}=\text{O}$). MS (EI^+) m/z (%) 237 (5), 119 (1), 105 (100), 77 (34).

2-(Phenylamino)acetophenones (**11a**,⁶² **11b**,⁶³ **11c**, and **11d**) were synthesized from 2-bromoacetophenone (Aldrich) by using a reported procedure.⁶²

2-(*m*-(Trifluoromethyl)phenylamino)acetophenone (11c**):** mp 142 °C. ^1H NMR (200 MHz, CDCl_3) δ 4.63 (d, $J = 4$ Hz, 2H), 5.18 (bs, 1H), 6.87 (d, $J = 8$ Hz, 1H), 6.88 (s, 1H), 6.99 (d, $J = 8$ Hz, 1H), 7.30 (t, $J = 8$ Hz, 1H), 7.49–7.65 (m, 3H), 8.04 (d, $J = 7$ Hz, 2H). ^{13}C NMR (50 MHz, CDCl_3) δ 49.83 (CH_2), 108.74, 114.16, 116.30, 127.79, 128.96, 129.70, 134.07 (aromatic), 124.33 (q, $J = 272$ Hz, CF_3), 131.69 (q, $J = 31$ Hz, $\text{C}-\text{CF}_3$), 134.61 ($\text{C}-\text{C}=\text{O}$), 147.16 ($\text{C}-\text{NHCH}_2$), 194.34 ($\text{C}=\text{O}$). MS (EI^+) m/z (%) 279 (10), 260 (3), 174 (100), 145 (10), 127 (8), 105 (10), 77 (14).

2-(*p*-Cyanophenylamino)acetophenone (11d**):** mp 186 °C dec. ^1H NMR (200 MHz, CDCl_3) δ 4.63 (d, $J = 4$ Hz, 2H), 5.50 (bs, 1H), 6.68 (d, $J = 9$ Hz, 2H), 7.46–7.70 (m, 5H), 8.02 (d, $J = 7$ Hz, 2H). ^{13}C NMR (50 MHz, CDCl_3) δ 49.16 (CH_2), 99.56 ($\text{C}-\text{CN}$), 112.65, 127.81, 129.03, 133.83, 134.31 (aromatic), 120.22 (CN), 149.95 ($\text{C}=\text{O}$).

(62) Fourrey, J.-L.; Beauhaire, J.; Yuan, C. W. *J. Chem. Soc., Perkin Trans. 1* **1987**, 1841–1843.

(63) Prakash, O.; Rani, N.; Goyal, S. *Indian J. Chem.* **1992**, *31B*, 349–350.

NHCH₂), 193.62 (C=O). MS (EI⁺) *m/z* (%) 236 (12), 131 (100), 105 (20), 102 (11), 77 (23).

Electrochemistry. The cyclic voltammetry was performed with a PAR 173 potentiostat equipped with a PAR 179 plug-in and a PAR 175 signal generator. The output from the potentiostat was filtered by a PAR 189 selective amplifier in the low pass mode before being digitized and stored by a Tektronix TDS 620 oscilloscope. The frequency (in Hz) of the selective amplifier was adjusted to be one hundred times the scan rate (in V·s⁻¹).⁶⁴ Noise originating from the power lines (60 Hz) was reduced by triggering the signal generator and oscilloscope from a homebuilt phase-sensitive trigger unit (based on the design of Nielsen et al.⁶⁴) and averaging two consecutive scans. The baseline subtraction and calculation of E_p and $E_{p/2} - E_p$ from experimental LSV curves were done by using the procedure in ref 60.

The electrochemical cell contained 5 mL of solution purged by argon. The mercury working electrodes were made by electrolytically depositing mercury onto a platinum disk electrode with a diameter of 0.5 mm that was sealed into glass.⁶⁵ The counter electrode was a platinum wire. The reference electrode was made by immersing a silver wire into DMF containing 0.1 M TEAP in a glass tube with a sintered glass bottom made according to Moe.⁶⁶ The potential of the reference electrode was measured against the ferrocene/ferrocenium couple, Fc/Fc⁺, before and after each series of measurements.

Determination of E° Values for the Reversible Couples. Cyclic voltammograms (CV) that were the average of two consecutive CVs obtained by using the alternating phase trigger unit (described elsewhere in the Experimental Section) were used for the determination of the E° values. The switch potential was 200–300 mV more negative than the E° value of the compound, and the initial and final potentials of the voltage scan were 400–500 mV more positive than the E° value. The α -arylaminoacetophenones gave only one reversible couple in this potential range. The *iR*-compensation was adjusted to 96–98% of the oscillation value.

The E° values were calculated as the midpoint between the cathodic and anodic peak potentials. The measurements were repeated with a range of sweep rates that covered at least two orders of magnitude. This was done in order to ensure that the E° values were unaffected by kinetic shifts (at low sweep rates) or by uncompensated resistance (at high sweep rates). The final E° value was taken as the average of

(64) Nielsen, M. F.; Laursen, S. A.; Hammerich, O. *Acta Chem. Scand.* **1990**, *44*, 932–943.

(65) Nielsen, M. F.; Hammerich, O.; Parker, V. D. *Acta Chem. Scand.* **1986**, *B40*, 101–118.

(66) Moe, N. S. *Anal. Chem.* **1974**, *46*, 968.

at least four determinations, all independent of the sweep rate (within a 4–5 mV range). The above set of measurements were repeated on a different day for each compound with new solutions. The values reported in Table 2 are the average from two such sets of measurements. These values were always within 3–4 mV of each other.

Every series of measurements for each compound always started and ended with the determination of the E° value for the ferrocene/ferrocenium couple which was measured as described above for the α -arylaminoacetophenones. This was done in order to ensure that the potential of the reference electrode had drifted less than 2 mV during the experiment. The start potential calculated from the data collected by the digital oscilloscope was routinely compared to the value measured by a multimeter. The internal-scope calibration program was run if the two values deviated more than 3 mV.

Constant Current Coulometry. Constant current coulometry was performed on 50-mL solutions purged by argon. The cathode was a mercury pool and the anode was a platinum wire. The anolyte was separated from the catholyte by a horizontal sintered glass disk and a 3–4 mm thick layer of neutral aluminum oxide. The current was kept constant at 30 mA. The coulometry cell was also equipped with mercury, reference, and counter electrodes (as used for the CV experiments described above) in order to monitor the concentration of the substrate during the electrolysis from CV peak heights.⁶⁷ The number of F/mol consumed during the reduction process was calculated from the slope of a plot of the CV peak heights versus the number of coulombs passed through the solution. These plots were generally linear until approximately 70% of the α -aryloxyacetophenone had been converted.⁶⁷ The catholytes from the coulometry experiments were acidified with 25 μ L of acetic acid and analyzed either directly by HPLC (HP ODS Hypersil column, 5 μ m, 200 \times 2.1 mm; eluant, mixture of water and methanol) or by extracting a mixture of the acidified catholyte and 30–50 mL of water with ether and then analyzing the dried and concentrated extracts by GC-MS. Benzophenone were used as an internal standard and was added to the catholytes after the electrolysis.

Acknowledgment. We gratefully acknowledge the financial support from the Canadian Wood Pulp Network (D.D.M.W.) and the Danish Natural Science Research Council (M.L.A.).

JA954093+

(67) Hammerich, O.; Parker, V. D. In *Organic Electrochemistry, An Introduction and a Guide*, 3rd ed.; Lund, H., Baizer, M. M., Eds.; Marcel Dekker, Inc.: New York, 1991; pp 121–205.